Highly soluble Fe(III)-triethanolamine complex relevant for redox flow batteries

Aurore Lê, Didier Floner, Thierry Roisnel, Olivier Cador, Léa Chancelier, Florence Geneste

Highly soluble Fe(III)-triethanolamine complex relevant for redox flow batteries

Aurore Lê [a,b], Didier Floner [a*], Thierry Roisnel [c], Olivier Cador [a], Léa Chancelier [b] and Florence Geneste [a,*]

[a] Université de Rennes 1, ISCR, UMR-CNRS 6226, Campus de Beaulieu, 35042 Rennes cedex, France.
[b] Kemwatt, 11 allée de Beaulieu - CS 50837, F-35708 Rennes cedex 7, France.
[c] Centre de Diffractométrie X (CDIFX), Institut des Sciences Chimiques de Rennes, UMR6226 CNRS-Université de Rennes 1, Campus de Beaulieu, 35042 Rennes cedex, France.

ABSTRACT: Fe-triethanolamine is a promising candidate as anolyte for redox flow batteries (RFBs), owning to its low potential, high solubility and low cost. We report here a new dinuclear structure of this complex at solid state when prepared with a stoichiometric amount of triethanolamine and iron in basic medium, whereas more than two equivalents of ligands are usually used to prepare Fe-triethanolamine for RFBs application. We achieve a calibration curve to estimate Fe(III) concentration in solution and coulometric experiments highlight a one-electron reduction process per iron atom, corresponding to the reduction of the two Fe(III) atoms of the dinuclear complex into Fe(II). A solubility higher than 1.2 mol dm^{-3} can be reached for Fe-triethanolamine with the new synthesis proposed in this work. All-Fe alkaline RFBs implemented with Fe-triethanolamine exhibit good performances in terms of coulombic, voltage and energy efficiencies, and is stable over a hundred of cycles. A power density around 80-120

Corresponding authors.

* didier.floner@univ-rennes1.fr

* florence.geneste@univ-rennes1.fr

mW cm^{-2} is reached and the high solubility of Fe-triethanolamine allows the achievement of high volumetric capacities, superior to 10 Ah dm^{-3}.

Keywords: all-Fe battery, Fe complex, organometallic electrolyte, triethanolamine, volumetric capacities

1. Introduction

Triethanolamine (TEA) has been widely used as ligand owning to its tetradentate chelating character, low cost and commercial availability. Among the transition metals that have been tested for its complexation, iron has retained a lot of attention with applications ranging from the formation of biologically active metallated ionic liquids [1] and the production of pure iron oxide magnetite Fe_3O_4 by electrochemical deposition [2-5] to photocatalytic production of hydrogen in aqueous medium [6]. In addition, Fe(III)-triethanolamine (Fe(III)-TEA) exhibits a reversible Fe(III/II) system at a very low potential (-1.15 V *vs* Ag/AgCl) and a high solubility in alkaline medium, making it a very efficient reducing agent. Thus it has been used as an environmentally friendly mediator for indirect electroreduction of vat dyes such as indigo for industrial dyeing processes [7-12]. Another particularly attractive application of this interesting redox behaviour of Fe(III)-TEA is redox flow battery (RFB) [13-15]. This large-scale energy storage technology is well-adapted for renewable energies owning to power/energy independent sizing, low cost and high-efficiency. Its performances in terms of voltage and stability strongly depend on the involved redox couples. Thus, Fe(III)-TEA/Fe(II)-TEA has proved its efficiency as negative redox couple in RFBs, leading to high cell voltage. Concentrations raising 0.6 and 0.8 mol dm^{-3}

in Fe(III) salts have been reported [13]. To facilitate its implementation in RFBs, the Fe(III)-TEA complex has been synthesized *in situ* using more than 2 eq. of TEA per Fe atom [13-15]. Whereas its structure in solution is not known, the crystal structure of the complex corresponding to a protocol involving 2 eq. of TEA per Fe atom at solid state has been reported to be a mononuclear complex with an iron atom coordinated by two TEA ligands in a regular octahedral configuration [16, 17].

Herein, we report a new X-ray crystal structure of a Fe(III)-TEA complex prepared in basic medium at high concentrations using a stoichiometric amount of TEA. The oxidation state of iron atoms and the number of electrons transferred were determined. The performance of the complex in RFB was tested, underlining the interest of this high soluble complex to achieve high volumetric capacities.

2. Experimental

2.1. Materials

Iron(III) sulfate hydrate and triethanolamine (98%) were purchased from Alfa Aesar. Potassium sulfate was from Sigma Aldrich and sodium hydroxide from Acros Organics. All solutions were prepared with ultrapure water (18.2 MΩ, Millipore Simplicity).

2.2. Instrumentation

High resolution mass spectra (HRMS) were obtained with a Bruker Maxi 4G and a Thermo Fischer Scientific Q-exactive with an electrospray ionisation (ESI) at the Centre Régional de Mesures Physiques de l'Ouest (CRMPO) in Rennes. Elemental analysis was performed at the Centre Régional de Mesures Physiques de l'Ouest (CRMPO) in Rennes. Voltammetric

experiments were carried out using a BioLogic SP150 potentiostat/galvanostat apparatus. A glassy carbon electrode (0.071 cm^2), a platinum wire auxiliary electrode, and a silver/silver chloride reference electrode (Ag/AgCl) were used in a standard three-electrode configuration for cyclic voltammetry experiments. Linear Sweep Voltammetry (LSV) at a 0.0314 cm^2 gold rotating disc electrode (Metrohm) was performed at 20 mV s^{-1} scan rate with a rotation rate of 1000 rpm, under a dinitrogen atmosphere.

2.3. Synthesis of Fe(III)-TEA complex.

100 g (< 0.25 mol) iron(III) sulfate hydrate ($Fe_2(SO_4)_3$, xH_2O) were dissolved in 200 cm^{-3} water leading to a dark red solution. 78 g (0.52 mmol) triethanolamine were then added under stirring. To this solution, 140 g (2.5 mol) potassium hydroxide dissolved in a minimum of water were added. The dark solution was stirred for 30 min and K_2SO_4 formed was then filtered on Buchner funnel. The precipitate was rinsed with water and the filtrate was collected and added to the previously filtered solution. It was then filtered again on a fritted glass and completed to 500 mL with water in a volumetric flask. This synthesis protocol led to a concentration of 0.84 mol dm^{-3} of Fe-TEA, according to the calibration curve obtained by linear sweep voltammetry at a rotating disk electrode.

Crystals were grown by slow evaporation of water. They were rinsed with cold water and dried at air during several days (around 10 g of crystals for 100 cm^{-3} of solution).

The crystals were crushed and the resulting powder was dried at a vacuum pump at 70-80°C during three days, to dehydrate the substrate. Results in elemental analysis correspond to the μ-oxo bis(TEA) diiron complex with three molecules of water. Elemental analysis measurements (%) Found, C, 26.10; H, 5.39; N, 4.89 Theoretical values calculated for $C_{12}H_{30}N_2O_{10}K_2Fe_2$: C, 26.10; H, 5.48; N, 5.07%).

Experiments that have been performed in H_2O + 0.01 M KOH on a Bruker Maxi 4G by electrospray ionization (ESI) gave the dimer Fe-O-Fe as the main ion: HRMS (ESI): *m/z* calculated for $C_{12}H_{24}N_2O_7K_3Fe_2$ $[(LFe)_2O+3K]^+$: 536.9190; found, 536.9188.

2.4. Magnetic susceptibility

The magnetic susceptibility measurements were performed on solid polycrystalline sample with a Quantum Design MPMS-XL SQUID (Superconducting QUantum Interference Device) magnetometer between 2 and 300 K in an applied magnetic field of 0.5 T for temperatures in the range 2-20 K and 1 T for temperatures between 20 and 300 K. These measurements were all corrected for the diamagnetic intrinsic contribution as calculated with Pascal's constants and for the diamagnetism of the sample holder measured separately.

Dimer magnetic model [18]:

$$H = -J\,\boldsymbol{S_1}\cdot\boldsymbol{S_2} \qquad \text{(eq. 1)}$$

$$\chi_M T = \frac{2Ng^2\beta^2}{k}\,\frac{\exp\left(\frac{J}{kT}\right)+5\exp\left(\frac{3J}{kT}\right)+14\exp\left(\frac{6J}{kT}\right)+30\exp\left(\frac{10J}{kT}\right)+55\exp\left(\frac{15J}{kT}\right)}{1+3\exp\left(\frac{J}{kT}\right)+5\exp\left(\frac{3J}{kT}\right)+7\exp\left(\frac{6J}{kT}\right)+9\exp\left(\frac{10J}{kT}\right)+11\exp\left(\frac{15J}{kT}\right)} \qquad \text{(eq. 2)}$$

2.5. Coulometry

The reduction of Fe(III)-TEA (solution prepared as reported above) was performed under argon in a home-made flow cell (Fig. 1) [19].

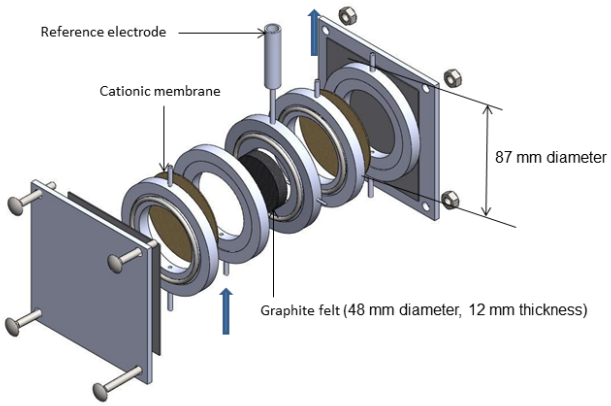

Fig. 1. Schematic diagram of the flow electrochemical cell used for coulometry experiments. The blue arrows are showing the direction of the electrolyte flow.

To ensure a good homogeneity of the potential distribution in the three dimensional working electrode consisting of a graphite felt (Recycled Vein Graphite RVG 4000 supplied by Mersen, France*;* 48 mm diameter, 12 mm thickness), the felt was located between two interconnected DSA counter-electrodes (dimensionally stable anodes, AC-2004, supplied by ECS International Electro Chemical Services, France). The compartments were separated by cationic exchange membranes (Ionac 3470 – Lanxess SAS, Courbevoie, France). The reference electrode (saturated calomel electrode, SCE) was positioned in the middle of the graphite felt and the electrolysis was performed at constant current intensity ranging from 50 to 400 mA in order to maintain a potential at the working electrode higher than -1.2 V *vs.* SCE. These chronoamperometry experiments were controlled by a BioLogic SP150 potentiostat/galvanostat apparatus. 100 cm^{-3} of the Fe(III)-TEA solution carefully degassed with dinitrogen percolated the porous electrode with recycling at a flow rate of 13 cm^3 min^{-1} monitored by a Gilson minipuls 3 peristaltic pump (Middleton, WI, USA). The cathodic reduction of Fe(III)-TEA was followed by LSV at a 0.0314 cm^2 gold rotating disk electrode. The number of electrons was calculated using the values

obtained at the end of the electrolysis to be sure to have a proportionality between the diffusion-limited current and the concentration of Fe(III) atoms, using the following equation:

$$n_{e-} = \frac{Q_{exp}}{(C_{initial} - C_{final})VF}$$

with Q_{exp} the charge passed, V the solution volume, F the Faraday's constant, $C_{initial}$ the initial concentration = 0.84 mol dm^{-3} and C_{final} the concentration of remaining Fe(III)-TEA estimated from the calibration curve.

2.6. RFB performance

RFB tests were performed using a home-made cell containing graphite felt electrodes (square cuboid 50 × 50 × 4.6 mm with 35% compression of the thickness leading to 95.5% porosity) with a geometrical surface area of 25 cm^2, composite graphite current collectors and cationic ion-exchange membrane. The positive and negative electrolytes (20 cm^{-3}) were pumped at a flow rate of 150 cm^3 min^{-1} (linear flow velocity: 3.1 cm s^{-1}) through KNF Pump (NF1-100KT-18S). The battery was operated through a Bio-Logic SP150 potentiostat with a 20 A booster.

2.7. NMR

NMR spectra were recorded on a Bruker AH300 FT spectrometer. After 110 cycles, a sample of the positive electrolyte was taken, evaporated and dried under vacuum. The solid was dissolved in D_2O until saturation was reached. The sample was filtered and then analyzed.

3. Results and discussion

3.1. Synthesis and characterization of the Fe-TEA complex

The Fe-TEA complex was prepared by reaction of $Fe_2(SO_4)_3$ (around 1 mol dm^{-3}) with around 2 eq. of TEA (i.e. around 1 eq. per Fe(III) atom) in water before adding a solution of KOH (pH close to 14). It is interesting to note that the use of KOH instead of NaOH as reported before [13-15] allows reaching concentrations higher than 1.2 mol dm^{-3} in Fe(III) salts. Slow volume reduction afforded large dark brown crystals, which were suitable for X-ray crystallographic study (Fig. 2).

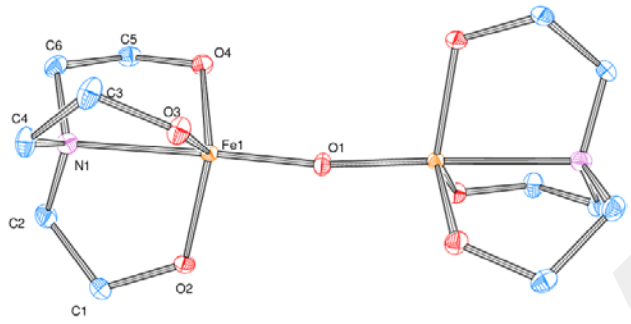

Fig. 2. Structure of the Fe-TEA complex showing 50% probability thermal ellipsoids and atom-labelling scheme. Hydrogen atoms, K^+ and H_2O molecules are omitted for clarity. Selected interatomic distances (Å) and angles (deg.): Fe…Fe, 3.6083(8); Fe1 - O1, 1.8121 (5); Fe1 - O4, 1.920 (2); Fe1- O2, 1.9445 (19); Fe1- O3, 1.9472 (19); Fe1- N1, 2.280 (2); Fe-O-Fe, 169.28(17). (CCDC 1517808 see supplementary material).

The molecular formula was found to be $C_{12}H_{46}Fe_2K_2N_2O_{18}$, corresponding to a molecular weight of 696.41 g mol^{-1}. Plots of the two anions with the K^+-oxygen interaction network involving 11 water molecules are included in supplementary material. The complex in solid state consists in a μ-oxo bis(TEA) diiron core and each iron is tetracoordinated by a TEA ligand. Two iron(III) atoms having trigonal bipyramidal coordination geometry are bridged by one oxygen atom, with

a Fe-Fe distance of 3.6083(8) Å and a Fe-O-Fe angle of 169.28(17)°, close to the linearity. Right side of the complex is generated from asymmetric unit content and applying the 1-x,y,-z+1/2 symmetry operator.

The structure of the complex was also confirmed by mass spectrometry and elemental microanalysis.

Temperature variable magnetization measurements have been used to verify the oxidation state, and spin state of iron solid state. At room temperature, $\chi_M T$ (χ_M the molar magnetic susceptibility and T the temperature in Kelvin) is equal to 8.75 cm^3 K mol^{-1} which perfectly fits with the expected value for two uncoupled high spin Fe(III) (S=5/2) spins (8.75 cm^3 K mol^{-1} with g=2) (Fig. 3) [18].

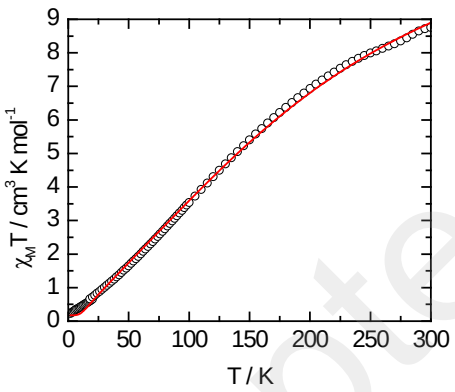

Fig. 3. Temperature variation of $\chi_M T$ between 2 and 300 K (circles) with the best fitted curve (red line) with the model exposed in text [18].

$\chi_M T$ decreases monotonically on cooling to reach 0.22 cm^3 K mol^{-1} at 2 K. The experimental curve can be reproduced with a dimer model featuring superexchange interaction between the two Fe(III) spins ($H=-J\ S_1 \cdot S_2$) through water molecule [18]. The best fit with the analytical

expression exposed in the experimental part incorporating a very small amount of paramagnetic impurities (0.2 cm^3 K mol^{-1}, g=2.07 and J=-31 cm^{-1}) is represented on Fig. 3.

3.2. Electrochemical characterization of Fe-TEA

The Fe-TEA solution, prepared according to our protocol was diluted in 1 mol dm^{-3} KOH solution and analyzed by cyclic voltammetry (Fig. 4).

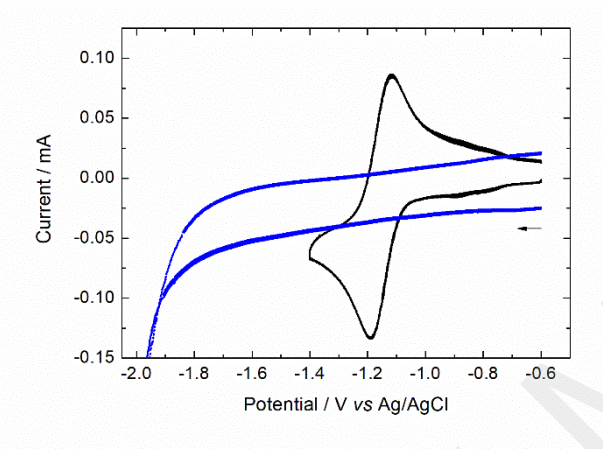

Fig. 4. Cyclic voltammogram of Fe-TEA (—) prepared according to our protocol and diluted in 1 mol dm^{-3} KOH solution (10^{-3} mol dm^{-3} of Fe) on a 0.071 cm^2 glassy carbon electrode. Blank in 1 mol dm^{-3} KOH solution (—). Scan rate 100 mV s^{-1}.

A reversible system at -1.15 V *vs* Ag/AgCl is obtained, with a difference between anodic and cathodic peaks around 70 mV, showing that the system corresponds to one electron exchange ($Fe^{III/II}$). The stability of the Fe-TEA solution prepared according to our protocol was also estimated by cyclic voltammetry after six-month storage at room temperature (Fig. S1 in supplementary material). No degradation of the Fe-TEA complex could be observed.

To estimate the real concentration of Fe-TEA complex in solution, a calibration curve was established by Linear Sweep Voltammetry (LSV) at a rotating disk electrode using a solution of

Fe-TEA prepared from isolated crystals (Fig. S2 in supplementary material). The concentration of the initial solution in Fe(III) complexed by TEA was calculated by using the following equation:

$$C_{Fe(III)} = \frac{m}{2M}$$

With *m*, the mass of crystals (3.5 g) and *M* the molecular mass estimated from X-ray analysis (696.41 g mol^{-1}).

The diffusion-limited current was proportional to the concentration of Fe-TEA in the range 0.01 to 0.1 mol dm^{-3} (Fig. 5), whereas the linearity was lost at higher concentrations (Fig. S3 in supplementary material).

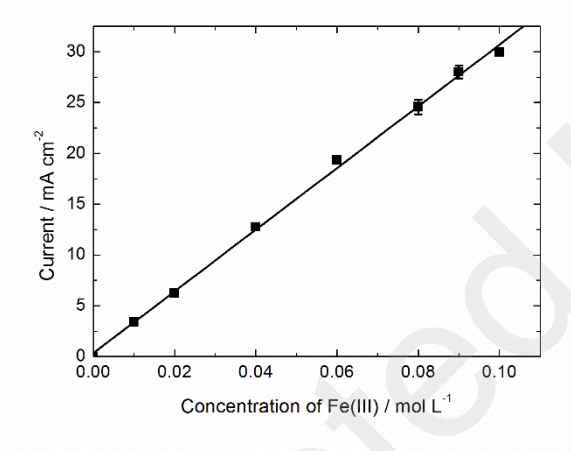

Fig. 5. Plots of current vs. concentration in Fe(III) constructed from LSV analysis at a gold rotating disk electrode of solutions of Fe(III) prepared by dilution of a 0.1 mol dm^{-3} Fe(III) solution obtained from isolated crystals of Fe(III)-TEA (3.5 g) dissolved in 1 mol dm^{-3} KOH solution saturated with K_2SO_4. Dilutions were performed with the same 1 mol dm^{-3} KOH solution saturated with K_2SO_4. Error bars are based on 2 measurements.

LSV analysis of a solution of Fe-TEA (around 1 mol dm^{-3}) prepared from reaction of $Fe_2(SO_4)_3$ with TEA and diluted ten times by a 1 mol dm^{-3} KOH solution saturated with K_2SO_4 gave rise to

a diffusion-limited current of 25.8 mA cm^{-2}. According to the calibration curve depicted in Fig. 5, it corresponds to a concentration in complexed Fe(III) of 0.84 mol L^{-1}.

Another important point for RFB application is the number of electrons that can be exchanged by the Fe-TEA complex. Indeed, the formation of a mixed valence compound $[(TEA)Fe(III)OFe(II)(TEA)]^{3-}$ has been previously mentioned for Fe-TEA synthesized with more than 2 eq. of TEA per Fe atom [13]. This dinuclear compound would be the oxidized form of $[(\mu\text{-}O)(Fe(TEA))_2]^{4-}$, resulting in a one electron process per dinuclear complex instead of two. To investigate the number of electrons exchanged during the reduction of the Fe-TEA complex prepared according to our procedure, bulk electrolyses were carried out in a flow electrochemical cell (Fig. 1). Coulometry was performed on a solution of 0.84 mol dm^{-3} Fe-TEA in a KOH solution (pH=14) saturated with K_2SO_4 at constant current intensity ranging from 50 to 400 mA in order to maintain a potential at the working electrode higher than -1.2 V *vs.* SCE. The same Fe-TEA solution was reoxidized at air after reduction and used for coulometry experiments three times more. The reaction was followed by LSV at a rotating disk electrode to estimate the concentration of remaining Fe-TEA in the solution (Fig. S4 in supplementary material). In the experimental conditions used to reduce Fe(III) into Fe(II), the reduction of Fe(II) into Fe(0) was avoided as evidenced by the stability of the total current during the electrolysis (Fig. S5 in supplementary material). A value of 0.90 ± 0.08 electrons per Fe atom was found, corresponding to the reduction of the two Fe(III) atoms of the dinuclear complex into Fe(II).

3.3. Battery performance

The performance of the all-Fe alkaline RFB with 0.4 mol dm^{-3} $K_4[Fe(CN)_6]$ in 1 mol dm^{-3} KOH/NaOH (75:25) positive electrolyte and 0.5 mol dm^{-3} Fe-TEA in 1 mol dm^{-3} KOH/NaOH

(80:20) negative electrolyte was first evaluated by a charge-discharge test with a charging protocol of constant current density at 40 mA cm^{-2}, followed by a constant voltage (CV) step at 1.5 V (Fig. 6a). The initial coulombic efficiency (CE), voltage efficiency (VE) and energy efficiency (EE) found to be 92, 79 and 71% respectively, are in agreement with previous results (93, 78, 73%, respectively) reported for this type of battery using 0.2 mol dm^{-3} of $K_4[Fe(CN)_6]$ and Fe-TEA [14]. Fig. 6b shows the cycling volumetric capacity and efficiencies curves over 110 cycles, corresponding to 57h, at a current density of 40 mA cm^{-2}.

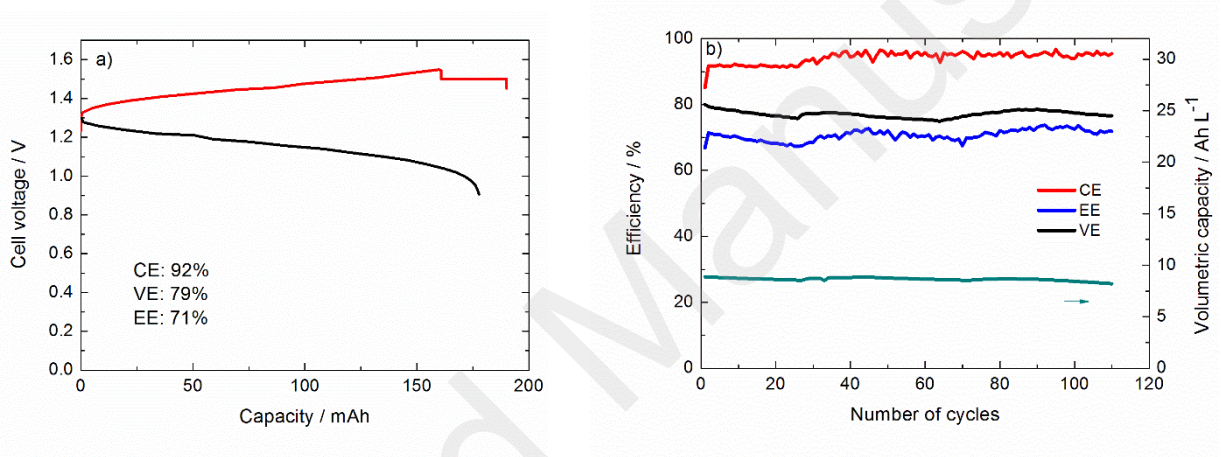

Fig. 6. a) Cell voltage curve of a charge-discharge test of an all-Fe alkaline RFB with 0.4 mol dm^{-3} $K_4[Fe(CN)_6]$ in 1 mol dm^{-3} KOH/NaOH (75:25) positive electrolyte and 0.5 mol dm^{-3} Fe-TEA in 1 mol dm^{-3} KOH/NaOH (80:20) negative electrolyte (CC: 40 mA cm^{-2}; CV 1.5 V) b) Coulombic efficiency (CE), voltage efficiency (VE), energy efficiency (EE) and volumetric capacity *vs* number of cycles.

The efficiencies were stable with the CE ranging from 92 to 97.5%, the VE higher than 74% and the EE around 70%. These values were close to those previously reported for an all-Fe alkaline RFB, although the CE was significantly higher [14]. Interestingly, the volumetric capacity (around 8.5 Ah dm^{-3}) was the double of the value previously reported [14] with a concentration

of Fe-TEA and $K_4[Fe(CN)_6]$ of 0.2 mol dm^{-3}. This result was expected since the concentration of $K_4[Fe(CN)_6]$ is the double for our all-Fe alkaline battery. It clearly highlights the interest of this new synthesis of Fe-TEA, allowing an improvement of the solubility of the complex in the electrolyte medium. Polarization curves were plotted to evaluate the power density of the RFB during cycling (Fig. 7).

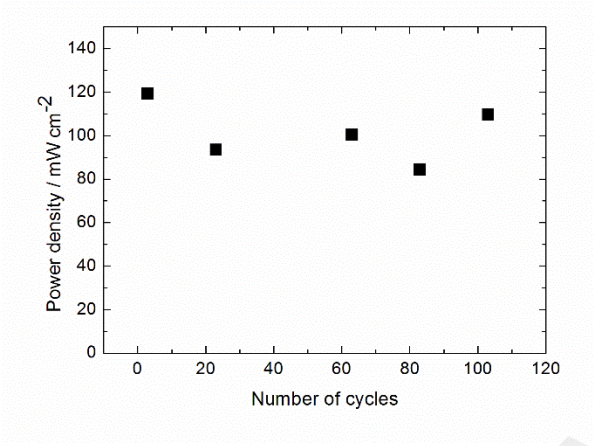

Fig. 7. Maximum power density *vs* number of cycles obtained by polarization curves performed at a 50% state of charge (SOC).

The values ranged between 84 to 119 mW cm^{-2} (for 50% state of charge), close to that of traditional all-Fe alkaline RFB (around 120 mW cm^{-2}) [20]. Then the volumetric capacity of the battery was improved taking advantage of the high solubility of Fe-TEA allowed by the new synthesis reported in this work. The performance of the all-Fe alkaline battery with 0.775 mol dm^{-3} $K_4[Fe(CN)_6]$ in 1 mol dm^{-3} KOH/NaOH (50:50) positive electrolyte and 1.1 mol dm^{-3} Fe-TEA in 2 mol dm^{-3} KOH/NaOH (50:50) negative electrolyte was evaluated. The initial and cycling efficiencies over 50 cycles (Fig. 8a,b) are similar to those obtained with lower concentrations (CE ~ 93%, VE > 74% and EE ~ 70%).

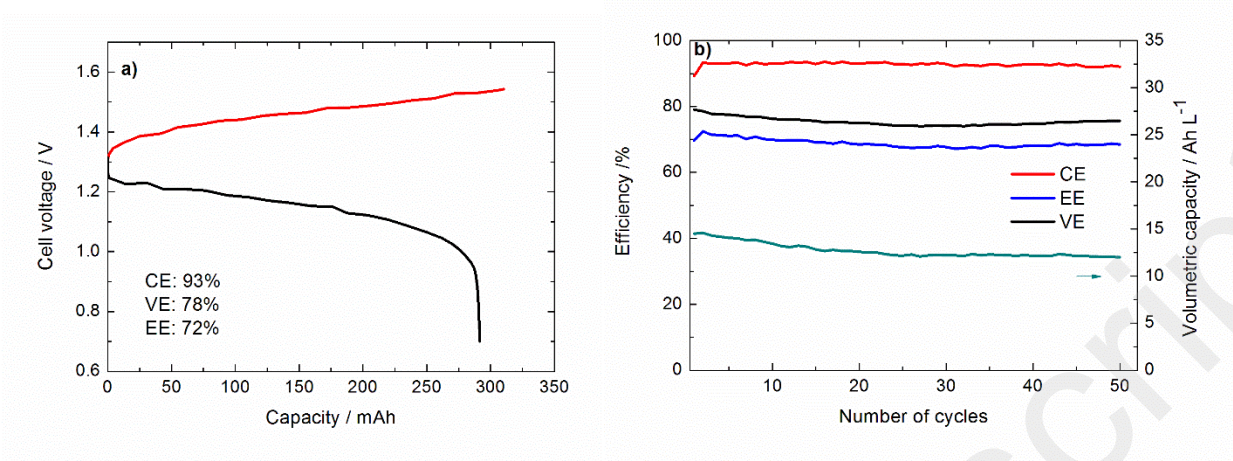

Fig. 8. a) Cell voltage curve of a charge-discharge test of an all-Fe alkaline RFB with 0.775 mol dm^{-3} $K_4[Fe(CN)_6]$ in 1 mol L^{-1} KOH/NaOH (50:50) positive electrolyte and 1.1 mol dm^{-3} Fe-TEA in 2 mol dm^{-3} KOH/NaOH (50:50) negative electrolyte at 40 mA cm^{-2} b) Coulombic efficiency (CE), voltage efficiency (VE), energy efficiency (EE) and volumetric capacity *vs* number of cycles.

The power density estimated during the cycling (Fig. 9) ranged between 101 and 117 mW cm^{-2} (for 50% state of charge). The initial volumetric capacity was around 14 Ah dm^{-3}, as expected for a $K_4[Fe(CN)_6]$ concentration of 0.775 mol dm^{-3}. This value slightly decreased during the first 20 cycles and stabilized around 12 Ah dm^{-3}. The decrease of the volumetric capacity could be due to different factors such as water transfer, species equilibrium or internal resistance but no significant cross-over of Fe-TEA was observed (Fig. S6 in supplementary material). Such volumetric capacity is high for redox flow batteries based on metallic complexes and/or organic redox species. For example, values around 4 Ah dm^{-3} have been reported for all-Fe alkaline batteries [20], up to 1.9 Ah dm^{-3} for quinone based batteries and from 1.34 to 5.36 Ah dm^{-3} [21] for batteries with flavin solubilized in hydrotropic agent [22].

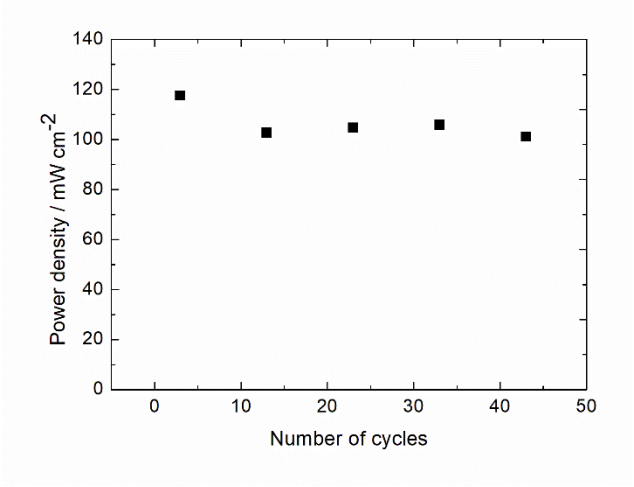

Fig. 9. Maximum power density *vs* number of cycles obtained by polarization curves performed at a 50% state of charge (SOC) for an all-Fe alkaline RFB with 0.775 mol dm^{-3} $K_4[Fe(CN)_6]$ in 1 mol dm^{-3} KOH/NaOH (50:50) positive electrolyte and 1.1 mol dm^{-3} Fe-TEA in 2 mol dm^{-3} KOH/NaOH (50:50) negative electrolyte.

4. Conclusions

In conclusion, the formation of a Fe-TEA complex at high concentrations (> 1.2 mol dm^{-3}) was achieved thanks to a simple new synthetic protocol easily scaled up to a larger scale. The compound was characterized in terms of structure of the complex at solid state and oxidation degree of the Fe atom, showing a μ-oxo dimer containing two Fe(III) atoms. Electrochemical methods were applied to establish the exact concentration of iron after synthesis and the number of electrons exchanged during the reduction process, showing that the Fe-TEA complex exchange 1 electron per Fe atom. The RFB results are very promising since it exhibited good performances in terms of power density (80-120 mW cm^{-2}) and stability with a volumetric capacity (around 12 Ah dm^{-3}) that is high for redox flow batteries based on metallic complexes and/or organic redox species.

Appendix A. Supplementary data

Structural characterization, Fig. S1 to S6.

Acknowledgment

A. Lê thanks ANRT and Kemwatt for her Ph.D grant.

References

[1] I.A. Ushakov, V.K. Voronov, S.N. Adamovich, R.G. Mirskov, A.N. Mirskova, The NMR study of biologically active metallated alkanol ammonium ionic liquids, J. Mol. Struct., 1103 (2016) 125-131.

[2] E.A. Kulp, H.M. Kothari, S.J. Limmer, J. Yang, R.V. Gudavarthy, E.W. Bohannan, J.A. Switzer, Electrodeposition of Epitaxial Magnetite Films and Ferrihydrite Nanoribbons on Single-Crystal Gold, Chem. Mater., 21 (2009) 5022-5031.

[3] H.M. Kothari, E.A. Kulp, S.J. Limmer, P. Poizot, E.W. Bohannan, J.A. Switzer, Electrochemical deposition and characterization of Fe3O4 films produced by the reduction of Fe(III)-triethanolamine, J. Mater. Res., 21 (2006) 293-301.

[4] C. Goujon, T. Pauporte, C. Mansour, S. Delaunay, J.L. Bretelle, Electrochemical Deposition of Thick Iron Oxide Films on Nickel Based Superalloy Substrates, Electrochim. Acta, 176 (2015) 230-239.

[5] S. Saadat, J. Zhu, D.H. Sim, H.H. Hng, R. Yazami, Q. Yan, Coaxial Fe_3O_4/CuO hybrid nanowires as ultra fast charge/discharge lithium-ion battery anodes, J. Mater. Chem. A, 1 (2013) 8672-8678.

[6] J. Dong, M. Wang, X. Li, L. Chen, Y. He, L. Sun, Simple Nickel-Based Catalyst Systems Combined With Graphitic Carbon Nitride for Stable Photocatalytic Hydrogen Production in Water, ChemSusChem, 5 (2012) 2133-2138, S2133/2131-S2133/2129.

[7] Y.h. Xu, H.f. Li, C.p. Chu, P. Huang, C.a. Ma, Indirect Electrochemical Reduction of Indigo on Carbon Felt: Process Optimization and Reaction Mechanism, Ind. Eng. Chem. Res., 53 (2014) 10637-10643.

[8] M.A. Kulandainathan, A. Muthukumaran, K. Patil, R.B. Chavan, Potentiostatic studies on indirect electrochemical reduction of vat dyes, Dyes Pigm., 73 (2006) 47-54.

[9] T. Bechtold, E. Burtscher, G. Kuhnel, O. Bobleter, Electrochemical reduction processes in indigo dyeing, J. Soc. Dyers Colour., 113 (1997) 135-144.

[10] T. Bechtold, E. Burtscher, A. Turcanu, O. Bobleter, Multi-cathode cell with flow-through electrodes for the production of iron(II)-triethanolamine complexes, J. Appl. Electrochem., 27 (1997) 1021-1028.

[11] T. Bechtold, E. Burtscher, A. Amann, O. Bobleter, Alkali-stable iron complexes as mediators for the electrochemical reduction of dispersed organic dyestuffs, J. Chem. Soc., Faraday Trans., 89 (1993) 2451-2456.

[12] T. Bechtold, E. Burtscher, D. Gmeiner, O. Bobleter, The redox-catalyzed reduction of dispersed organic compounds. Investigations on the electrochemical reduction of insoluble organic compounds in aqueous systems, J. Electroanal. Chem. Interfacial Electrochem., 306 (1991) 169-183.

[13] N. Arroyo-Curras, J.W. Hall, J.E. Dick, R.A. Jones, A.J. Bard, An Alkaline Flow Battery Based on the Coordination Chemistry of Iron and Cobalt, J. Electrochem. Soc., 162 (2015) A378-A383.

[14] K. Gong, F. Xu, J.B. Grunewald, X. Ma, Y. Zhao, S. Gu, Y. Yan, All-Soluble All-Iron Aqueous Redox-Flow Battery, ACS Energy Lett., 1 (2016) 89-93.

[15] Y.H. Wen, H.M. Zhang, P. Qian, H.T. Zhou, P. Zhao, B.L. Yi, Y.S. Yang, A study of the Fe(III)/Fe(II)-triethanolamine complex redox couple for redox flow battery application, Electrochim. Acta, 51 (2006) 3769-3775.

[16] B. Sen, R.L. Dotson, Characterization and studies of some triethanolamine complexes of transition and representative metals, J. Inorg. Nucl. Chem., 32 (1970) 2707-2716.

[17] A.A. Naini, V. Young, J.G. Verkade, New complexes of triethanolamine (TEA): novel structural features of $[Y(TEA)_2](ClO_4)_3 \cdot 3C_5H_5N$ and $[Cd(TEA)_2](NO_3)_2$, Polyhedron, 14 (1995) 393-400.

[18] O. Kahn, Molecular Magnetism, VCH: New York1993.

[19] F. Geneste, C. Moinet, Electrocatalytic oxidation of alcohols by a $[Ru(tpy)(phen)(OH_2)]^{2+}$-modified electrode, J. Electroanal. Chem., 594 (2006) 105-110.
[20] L.W. Hruska, R.F. Savinell, Investigation of factors affecting performance of the iron-redox battery, J. Electrochem. Soc., 128 (1981) 18-25.
[21] J. Cao, M. Tao, H. Chen, J. Xu, Z. Chen, A highly reversible anthraquinone-based anolyte for alkaline aqueous redox flow batteries, J. Power Sources, 386 (2018) 40-46.
[22] A. Orita, M.G. Verde, M. Sakai, Y.S. Meng, A biomimetic redox flow battery based on flavin mononucleotide, Nat. Commun., 7 (2016) 13230.